Corrosion Protection Performance and Spectroscopic Investigations of Soluble Conducting Polyaniline-Dodecylbenzenesulfonate Synthesized via Inverse Emulsion Procedure

Subrahmanya Shreepathi, Hung Van Hoang, Rudolf Holze

Corrosion Protection Performance and Spectroscopic Investigations of Soluble Conducting Polyaniline-Dodecylbenzenesulfonate Synthesized via Inverse Emulsion Procedure

Subrahmanya Shreepathi, Hung Van Hoang and Rudolf Holze*

Institut für Chemie, Technische Universität Chemnitz, AG Elektrochemie, D-09107 Chemnitz, Germany

* To whom correspondence should be addressed. E-mail: rudolf.holze@chemie.tu-chemnitz.de

Abstract

Corrosion protection performance of a completely soluble polyaniline-dodecylbenzenesulfonic acid salt (PANI-DBSA) on C45 steel has been studied with electrochemical impedance and potentiodynamic measurements. Chloroform is the most suitable solvent to process the pristine PANI-DBSA because of negligible interaction of the solvent with the polyaniline (PANI) backbone. An anodic shift in the corrosion potential (ΔE = ~70 mV), a decrease in the corrosion current and a significant increase in the charge transfer resistance indicate a significant anti-corrosion performance of the soluble PANI deposited on the protected steel surface. Corrosion protection follows the mechanism of formation of a passive oxide layer on the surface of C45 steel. *In situ* UV-Vis spectroscopy was used to investigate the differences in permeability of aqueous anions into PANI-DBSA. Preliminary results of electron diffraction studies show that PANI-DBSA possesses an orthorhombic type of crystal structure. An increase in the feed ratio of DBSA to aniline increases the tendency of aggregation of spherical particles of PANI obvious in transmission electron microscopy. PANI-DBSA slowly loses its electrochemical activity in acid free electrolyte without undergoing degradation.

Introduction

Conducting polymers, particularly polyaniline, have wide range of application in batteries, corrosion protection, sensors, electrooptic and electrochromic devices.[1 2 3] Over the last two decades many studies have focused on the corrosion protection of ferrous materials using emeraldine form of PANI.[4] Conducting polymer coatings are more tolerance to pinholes because of their passivation ability. The mechanism of corrosion protection, influence of the substrate preparation on corrosion protection and a direct comparison between PANI emeraldine salt and PANI emeraldine base have been reviewed in detail.[5] Previous reports also show that corrosion performance of PANI is affected by a number of parameters such as coating method, dopants used, electrolytes and their pH, etc.[5 6] Three main methods of coating PANI on steel are: direct electrochemical deposition, spin/drop coating of PANI from its solution/dispersion and polymer coating containing PANI as additive.[6] In the case of solution cast coating, usually the emeraldine base (EB) form of PANI dissolved in N-methyl pyrrolidone (NMP) is used which is further re-doped with different acids.[5] There are arguments regarding the commercial applicability of NMP cast PANI because they are not effective as well as impractical.[7] Counter ion induced solubility (secondary doping by camphorsulfonic acid or dodecylbenzenesulfonic acid in chloroform or xylene) of PANI has also been used to coat steel surfaces but such systems exhibit very poor efficiency of protection because of the presence of free acid molecules in the solution.[8]

Use of bulky organic acids such as camphorsulfonic acid (CSA) and dodecylbenzenesulfonic acid (DBSA) to protonate polyaniline (primary doping) has gained special attention following the report of Cao et al.[9] because of their enhanced solubility in common organic solvents. DBSA being a bulky molecule functions both as surfactant and dopant and its large non-polar chain facilitates the solubility of the resulting PANI. However, DBSA has poor water solubil-

ity and therefore a large volume of water is necessary to prepare anilinium-DBSA complex in aqueous solution.[10]

Sathyanarayana et al.[11,12] for the first time, have used benzoyl peroxide as the oxidizing agent in the polymerization of aniline in presence of various organic sulfonic acids as dopants. They reported that the organic peroxide (compared to the conventional ammonium persulfate) reduces the possibility of over-oxidation of PANI during exothermic reaction of aniline polymerization and the by-products of the oxidant can be easily removed by washing with acetone. Recently Sai Ram and Palaniappan [13] have also used benzoyl peroxide for the synthesis of polyaniline doped with mineral acids. Solubility of benzoyl peroxide in most of the organic solvents offers many solvent systems for the polymerization of aniline which yield PANI with different physicochemical properties and enhanced solubility.

We have recently investigated an inverse emulsion method for the synthesis of PANI-DBSA which is completely soluble in solvents such as chloroform. Spectroelectrochemical, electrochemical and morphological studies of the resulting polymer have been reported elsewhere.[14] In this paper, a pilot attempt towards the application of this soluble PANI has been carried out. PANI-DBSA dissolved in chloroform was drop-coated onto a steel electrode surface and its anti-corrosion performance is studied using electrochemical impedance measurements (EIM) and anodic polarization measurements. Influence of feed ratio of monomer to dopant on the corrosion protection is discussed. In addition, *in situ* UV-Vis spectroscopic and transmission electron microscopic investigations are also reported which gives a better understanding towards the ingress of aqueous anions into PANI film and its morphology.

Experimental

Chemicals.—Aniline (VEB Laborchemie Apolda, analytical grade) was distilled under reduced pressure and stored under nitrogen. DBSA (70 wt % in 2-propanol, 70 % solution, Aldrich), tetrabutylammoniumtetrafluoroborate (Bu_4NBF_4, Aldrich) and fluoroboric acid (as diethylether complex, Fluka) were used as received. Ultrapure (18 MΩ) water (Seralpur pro 90 C) was used. All other chemicals were analytical grade reagents and used as procured. Indium tin oxide (ITO) coated glass sheets (R = 20 Ω cm^{-2}) were supplied by MERCK. Mild steel cylinders (steel C45, Germany) of 1 cm height and 1.2 cm diameter were used in corrosion studies (Electrode area = 1.13 cm^2). Chemical composition of the C45 steel (wt %): C = 0.46, Si = 0.4, Mn = 0.65, Cr = 0.4, Mo = 0.1, Ni = 0.4 and others = 0.63.

Synthesis of PANI-DBSA.— Polymerization of aniline was carried out in an inverse emulsion medium composed of toluene+2-propanol (2:1) and water in the presence of DBSA using benzoyl peroxide as oxidant. Details of synthetic and purification procedure are described elsewhere.[14] Polyanilines with different mole ratios of DBSA to aniline have been prepared by keeping constant the oxidant-to-monomer ratio and by varying the concentration of DBSA. The polymer samples were labeled as TIP-5, TIP-6 and TIP-7 where the mole ratios of DBSA/aniline in the feed were 5:1, 7:1 and 10:1 respectively.

Characterization.— UV-Vis spectra were recorded using a Shimadzu 2100 PC spectrophotometer. A quartz cell of 1 cm path length and PANI dissolved in different solvents were used. For the *in situ* UV-Vis measurements, PANIs dissolved in $CHCl_3$ are drop coated on a clean ITO coated glass sheet subsequently used as working electrode. A quartz cell of 1 cm path length fitted with a platinum wire as counter electrode and saturated calomel electrode

(SCE) connected via salt bridge as a reference electrode served as a three-electrode cell. *In situ* measurements were carried out under ambient conditions.

Cyclic voltammograms (CVs) were recorded under nitrogen atmosphere in a three-electrode single compartment cell using a custom built potentiostat connected to a computer with an AD/DA converter. CVs were recorded in acetonitrile containing Bu_4NBF_4 as supporting electrolyte. PANI dissolved in $CHCl_3$ and drop coated onto a platinum sheet was used as working electrode after evaporation of the solvent. A platinum sheet counter electrode and a Ag/AgCl reference electrode (in acetonitrile containing Bu_4NBF_4) were used.

A combination of a Solartron SI1287 potentiostat and a SI1255 frequency response analyzer, both connected to a PC via IEE488.2 connections, was used to record electrode impedance data with a modulation amplitude of 5 mV in the frequency range of 0.1 Hz - 100 kHz. Evaluation of the impedance data was performed using equivalent circuits with the software packages Z-view and EQUIVCRT. Measurements were carried out in a three-electrode one compartment cell with a C45 steel disc working electrode, a gold sheet counter electrode and a saturated calomel reference electrode. PANIs dissolved in $CHCl_3$ were drop coated on the C45 steel discs which were previously polished with fine emery paper (P 1000) and with γ-Al_2O_3 (13 μm). Impedance measurements were carried out at ambient conditions in 3.5 % NaCl.

Anodic polarization measurements were carried out under ambient conditions in a three-electrode single compartment cell with a gold sheet counter electrode and a saturated calomel reference electrode using a Solartron SI1287 potentiostat connected to a computer via IEE488.2 connections. The working electrode was the C45 steel sample (PANI drop coated or uncoated) which was polished as described above prior to the measurements. 3.5 % (wt/wt) NaCl solution was used as corrosion environment and the measurements were carried at a scan rate of 5 mV/s.

Transmission electron microscopic (TEM) images were recorded on a Philips CM 20 FEG transmission electron microscope. The samples were prepared by depositing a drop of well diluted PANI in chloroform on a carbon (1 0 0) coated copper grid and dried in an oven at 50 °C for two hours.

Results and Discussion

Solution State UV-Vis Spectroscopy.— The clear green solution of PANI in the chloroform/2:1 mixture of toluene and 2-propanol can be spun or drop-coated as well-adhering films on various metallic and glass substrates. Electronic absorption spectra of PANI-DBSA dissolved in both solvents and the band assignments were discussed previously.[14] The influence of the feed ratio of DBSA/aniline on the UV-Vis spectra was discussed. Further details of polymer-solvent interactions and the voltammetric responses of chemically synthesized PANI-DBSA in aqueous acid free electrolytes containing different anions are discussed here.

Figure 1a shows UV-Vis spectra of TIP-5 dissolved in the 2:1 mixture of toluene+2-propanol at different concentrations of PANI. At lower concentrations of the polymer in the solution, a new band characteristic of PANI-EB appears at ~650 nm and the low energy polaron band (760-820 nm) shows a bathochromic shift (> 50 nm). The band at 345 nm indicative of the extent of conjugation in the polymer backbone undergoes a blue shift with decreasing concentration of PANI.

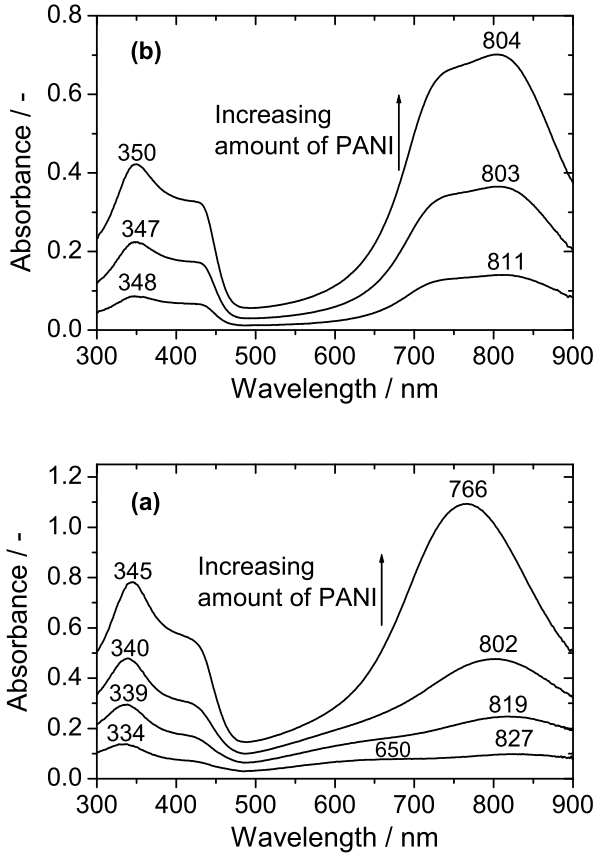

Figure 1. Solution state UV-Vis spectra of TIP-5 dissolved in 2:1 mixture of toluene + 2-propanol (a) and in chloroform (b).

However, such changes were not observed for PANI dissolved in chloroform except for a small red shift of the low energy polaron band (~ 7 nm). These observations reveal the interaction of 2:1 mixture of toluene+2-propanol with the polymer. The possible interaction between PANI and solvent in this case is hydrogen bonding between –N atoms of PANI and –OH group of the solvent. Athawale and coworkers[15] observed such interactions for acrylic acid doped polyaniline dissolved in *m*-cresol and in NMP where hydrogen bonding deprotonates the polymer chain. The ratio of absorbances of the bands at 330-350 nm and at 760-820 nm (A_{800}/A_{350}) reveals the extent of protonation of the polymer backbone and the influence of the solvent on protonation. When chloroform is used as a solvent, this ratio does not depend on the amount of PANI dissolved whereas in the case of 2:1 mixture of toluene+2-propanol, the ratio increases as the amount of PANI in the solution is increased. For example, the absorbance ratio of TIP-5 increases from 0.6 to 1.4 in a 2:1 mixture of toluene+2-propanol but shows a constant value of 1.6 in chloroform. A constant ratio suggests that PANI dissolved in chloroform retains protonation and thus its electrical properties in solution. However, varying the ratio of absorbance for PANI dissolved in 2:1 mixture of toluene+2-propanol proves its non-suitability for diluted solutions. Absorbance ratios of 1.1-1.2 were reported for polyaniline films on glass substrates and for PANI dispersions by Stejskal and Sapurina[16] without any further explanation.

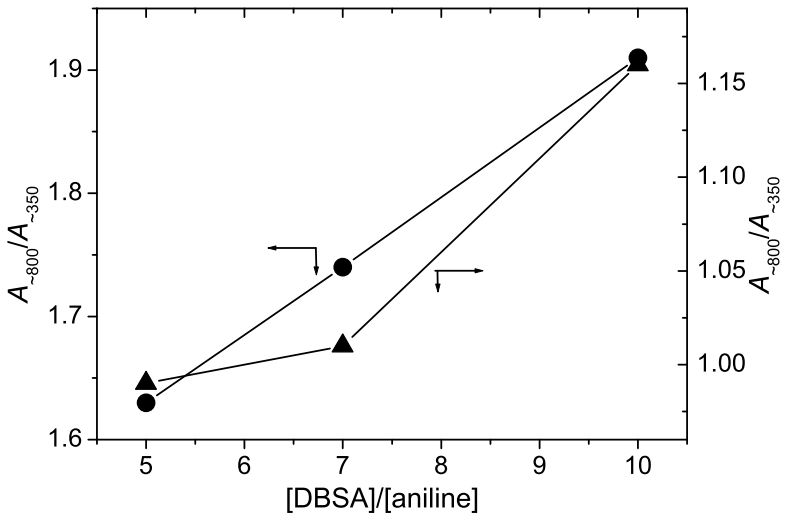

Figure 2. Plot of ratio of absorbances at ~ 820 to ~ 350 nm as a function of feed ratio of DBSA to aniline. Solution state spectra of PANI were recorded in chloroform (—●—) and in 2:1 mixture of toluene + 2-propanol (—▲—).

Figure 2 shows the plot of ratio of absorbances (A_{800}/A_{350}) as a function of feed ratio of DBSA to aniline. The absorbance ratio exhibits a linear increase with the feed ratio of DBSA to aniline when chloroform is used as solvent whereas a sharp increase is noticed when the feed ratio of DBSA to aniline is changed from 7 to 10 in case of the 2:1 mixture of toluene+2-propanol. Higher values of the ratio of absorbances for chloroform indicate the absence of solvent solute interaction.

In situ UV-Vis Spectroscopy in Acid Free Aqueous Electrolytes.—It is well known that PANI synthesized either chemically or electrochemically in presence of mineral acids does not exhibit redox activity at pH > 4.[17] However, the UV-Vis response of the chemically synthesized PANI doped with bulky organic dopant as a function of applied potential in acid free electrolytes has not been reported.

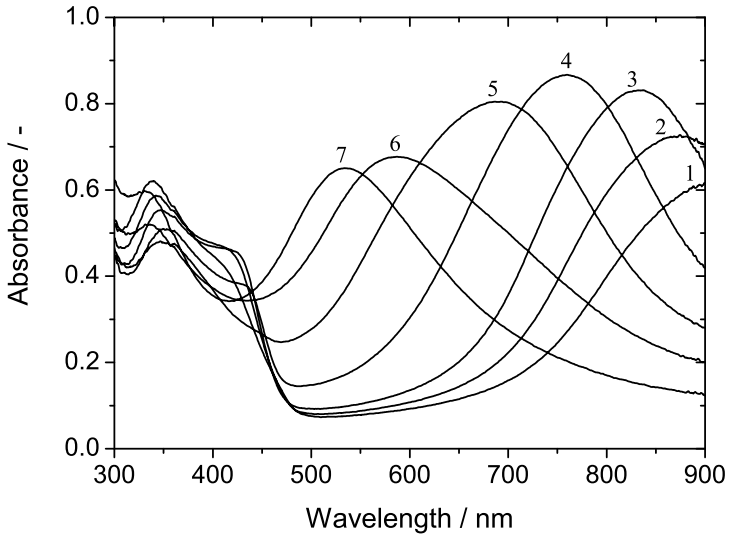

Figure 3. *In situ* UV-Vis spectra of drop coated film of TIP-5 recorded in 0.1 M KCl as a function of applied potential successively shifting to anodic direction. E_{SCE} (V): (1) –0.2 (2) 0, (3) 0.2, (4) 0.4, (5) 0.5, (6) 0.6 and (7) 0.8.

Figure 3 shows the *in situ* UV-Vis spectra of a drop coated film of TIP-5 as a function of applied potential successively shifted into anodic direction as recorded in 0.1 **M** KCl. The low energy band at ~800 nm shows a blue shift when the applied potential is increased from E_{SCE} = –0.2 to 0.8 V. Its absorbance increases up to E_{SCE} = 0.4 V and then decreases. The rapid blue shift of this band at E_{SCE} > 0.4 V can be attributed to the emeraldine to pernigraniline transformation. Such changes were also observed for PANI-DBSA films studied in 0.5 **M** H_2SO_4 but the oxidative transformation is observed at E_{SCE} > 0.6 V.[14] The band at ~400 nm exhibit maximum absorbance for E_{SCE} = 0.1 to 0.2 V indicating maximum protonation in this potential range.[18] This band is present even at E_{SCE} = –0.2 V where, generally, PANI exists in leucoemeraldine state which indicate that emeraldine-to-leucoemeraldine transformation of chemically synthesized PANI-DBSA takes place slowly. A decrease in the absorbance and a red shift is observed for the band at ~350 nm when the potential is increased from E_{SCE} = –0.2

to 0.5 V indicating a decreased conjugation caused by the protonation, an opposite trend is observed for E_{SCE} > 0.5 V. *In situ* UV-Vis spectra of PANI-DBSA films as a function of applied potential were also recorded during a cathodic sweep to complete a potential cycle. The spectrum shows only two bands at 330 nm and at 520-600 nm at all applied potentials. During an electrochemical oxidation, counter ions enter the PANI film whereas they are expelled from the film during reduction.[19] The insertion of Cl^- ions into the film during an anodic sweep is a slow process due to the repelling nature of long hydrophobic chain of DBSA and thus, UV-Vis responses of PANI film recorded in KCl are similar to those in H_2SO_4.

The *in situ* UV-Vis spectra measured in another acid free electrolyte solution containing relatively larger counter ions (SO_4^{2-}) reveal that anion exchange rate between PANI-DBSA and the electrolyte is influenced by the size of the anions. When larger anions are present in the solution (SO_4^{2-}), the bands corresponding to polaron transitions reappear during the negative going potential sweep (**Figure 4**).

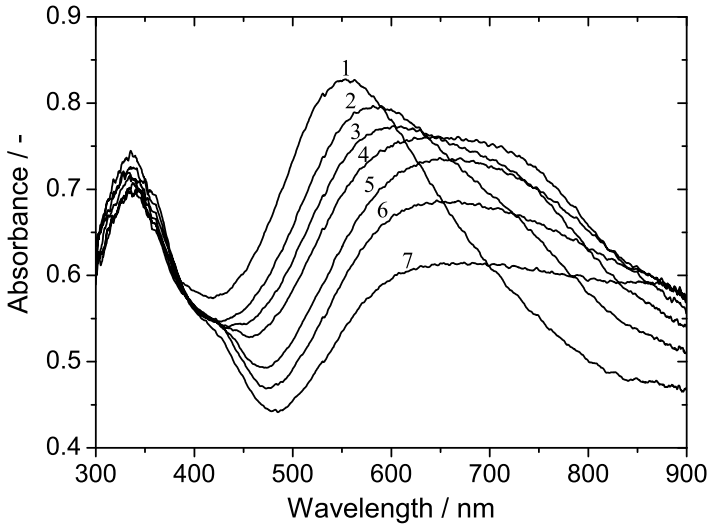

Figure 4. *In situ* UV-Vis spectra of drop coated film of TIP-6 recorded in 0.3 M Na_2SO_4 as a function of applied potential successively shifting to cathodic direction. E_{SCE} (V): (1) 0.8 (2) 0.4, (3) 0.3, (4) 0.2, (5) 0, (6) –0.1 and (7) –0.2.

It is clear from the figure that at E_{SCE} < 0.4 V, bands corresponding to protonated PANI-ES (~800 nm) are broad and overlapping with the band corresponding to PANI-EB (~600 nm). However, unlike in acidic electrolytes, electrochromic as well as electrochemical reversibility in terms of position and absorbance of the low energy band could be observed neither in KCl nor in Na_2SO_4 solution. The emeraldine to pernigraniline transformation during the anodic sweep in 0.3 **M** Na_2SO_4 is positively shifted to E_{SCE} > 0.5 V when compared to that in 0.1 **M** KCl. A PANI-DBSA film cycled in neutral electrolyte was washed with water, re-immersed in 0.5 **M** H_2SO_4 and cycled again to check for possible degradation/structural changes in neutral electrolytes. The UV-Vis response of the PANI film re-immersed in acid is similar to the one recorded for the fresh PANI film indicating the absence of structural modifications.

Cyclic Voltammetry.— Cyclic voltammograms (CVs) of PANI in acetonitrile containing 0.1 **M** Bu_4NBF_4 + 0.075 **M** HBF_4 show two pairs of well-defined redox waves similar to the ones observed with electrosynthesized PANI aqueous acids.[14] It is well established in the literature that in the absence of protonic acids (i.e. in a neutral electrolyte solution), PANI reversibly looses its redox activity and only one degenerated redox wave is observed.[20] CVs of TIP6 drop coated on the Pt-sheet electrode as a function of cycle number in acetonitrile containing 0.1 **M** Bu_4NBF_4 at a scan rate of 50 mV/s are shown in **Figure 5**.

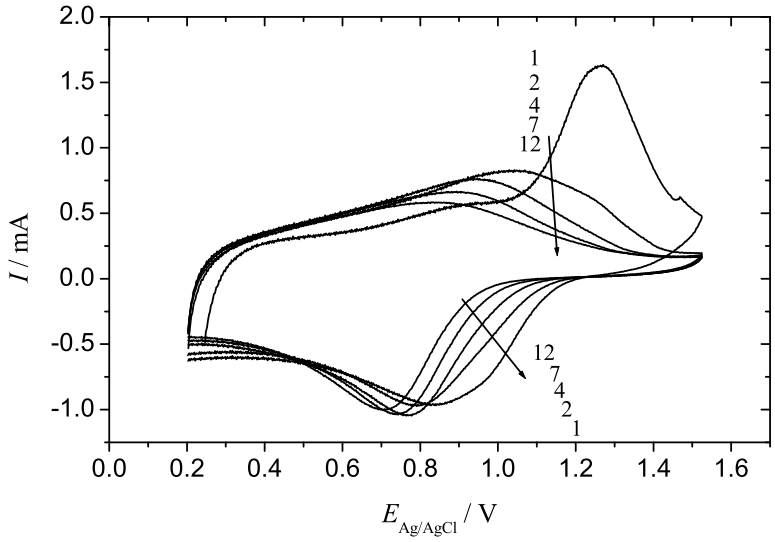

Figure 5. Cyclic voltammograms of TIP6 drop coated on Pt-sheet electrode in acetonitrile containing 0.1 M Bu_4NBF_4 recorded at 1st, 2nd, 4th, 7th and 12th cycle at a scan rate of 50 mV/s.

A peak in the region of $E_{Ag/AgCl}$ = 1.2-1.3 V in the first cycle is negatively shifted to $E_{Ag/AgCl}$ = 1.0-1.1 V in the second cycle and its peak current shows a steep decrease. During following cycles the position of this peak shifts further towards negative potentials, its peak current decreases gradually. Electrochemical activity of the PANI film is retained up to 30 cycles. As discussed in the preceding section on UV-Vis spectroscopy, such a gradual loss of electrochemical activity may be due to the slow exchange of bulky DBSA anions present in the film. Cycling of PANI coated platinum electrodes in acid free electrolyte does not bring irreversible structural modifications of the film which is confirmed by the presence of two well-defined redox peaks for a pre-treated (cycled in neutral electrolyte) PANI film in acetonitrile containing Bu_4NBF_4 + 0.075 **M** HBF_4.

Electrochemical Impedance Measurements (EIM).—EIM is frequently employed as a powerful tool to investigate the corrosion protection performance of organic coatings on a metal.[21] [22] [23] The Nyquist diagrams for the bare C45 steel electrode and PANI coated (with different feed ratios of DBSA to aniline) electrodes recorded at OCP in 3.5 % NaCl are shown in **Figure 6**.

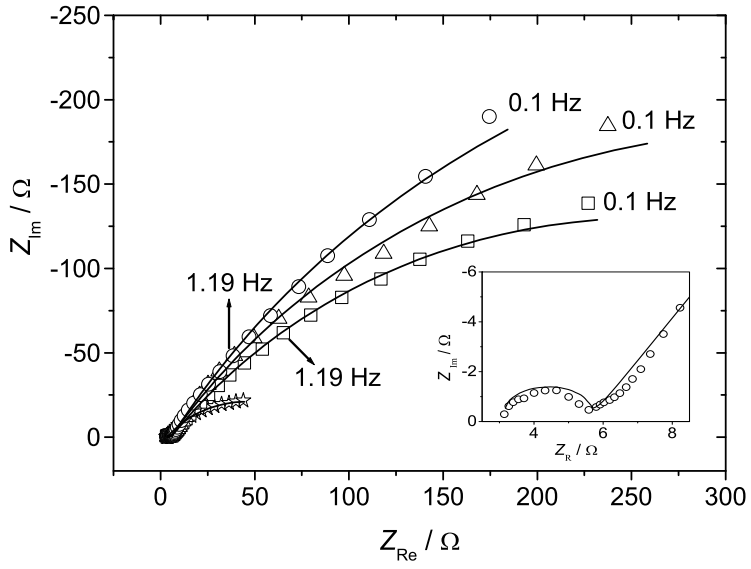

Figure 6. Nyquist diagrams of the bare C45 steel electrode (☆) and electrode coated with TIP-5 (Δ), TIP-6 (○) and TIP-7 (□) recorded at OCP in 3.5 % NaCl.. Solid lines indicate the curve fitting and the magnified portion of TIP-6 at high frequencies is shown in the inset.

The charge transfer resistance (R_{CT}), double layer capacitance (C_{DL}) and coating resistance (R_F) values determined via curve fitting of impedance data using Z-view software are given in **Table 1**.

Table 1. R_S, R_C, C_C, R_{CT} and C_{DL} values from impedance data for bare and PANI-DBSA coated C45 steel electrodes at various exposure times in 3.5 % NaCl.

Coating	T* / h	R_S / Ω	C_C / μF	R_F / Ω	C_{DL} / mF	R_{CT} / Ω
Uncoated	0	3.5	–	–	4.2	84.5
TIP-5	0	4.1	16.4	1.58	2.9	696
	24	4.5	3.9	1.69	3.2	650
	48	4.3	4.9	1.80	2.2	635
	72	4.3	4.9	1.76	2.5	378
TIP-6	0	4.5	11.9	1.12	4.3	880
	24	4.6	13.5	1.17	4.3	586
	48	4.6	10.6	1.18	4.1	559
	72	4.7	10.5	1.12	3.4	356
TIP-7	0	4.3	8.3	1.44	3.1	505
	24	3.4	1.9	0.75	1.6	449
	48	3.3	2.2	0.76	1.6	440
	72	4.6	4.7	1.13	2.7	425

* Measured at E_{OCP}

Two capacitive depressed semi-circles are present in the Nyquist diagrams. One of them at high frequencies is attributed to the electrical properties of the PANI film (R_F) and the other to processes occurring underneath the film (R_{CT}). The first loop can be visualized only after magnifying the high frequency range, both loops cannot be well resolved.[24 25] Such a behavior can be explained with an equivalent circuit containing a solution resistance (R_S), coating capacitance (C_C), double layer capacitance (C_{DL}), coating resistance (R_F) and charge transfer resistance (R_{CT}) as shown in **Figure 7**.[24 26]

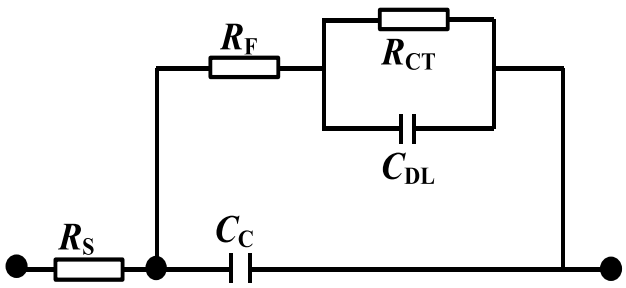

Figure 7. Equivalent circuit used to fit the impedance data of PANI-DBSA coated steel electrodes recorded in 3.5 % NaCl.

A good barrier allows very little current flow showing high resistance during impedance measurements.[27]

The protective effect of PANI-DBSA is immediately obvious as the R_{CT} value for PANI coated electrodes show significant increases compared to the bare C45 steel electrode (Table 1). Both resistance and capacitance values increase with increasing thickness of the PANI film, beyond a certain limit only a negligible further increase was observed. All values for PANIs reported in Table 1 are beyond this threshold. Repeated experiments show that the po-

larization resistance and thereby the corrosion efficiency is influenced by the amount of DBSA in the feed. TIP-6, where DBSA to aniline ratio is 7, shows relatively better corrosion protection. In conventional PANI coating, Cl^- ions and water can easily permeate due to the porosity of the film leading to a lower film resistance.[26] Bulk samples of PANI-DBSA show fibrillar, porous and compact film morphology when the mole ratio of DBSA to aniline is 5, 7 and 10 respectively.[14] However, R_{CT} values in our case could not be correlated to the bulk morphology of the polymer (TIP-6 with porous morphology shows higher R_{CT}) indicating the change in morphology during sample preparation which was later confirmed by TEM studies. The values of C_{DL} in Table 1 for PANI coated C45 steel electrodes lies in the range of 1.6 - 4 mF which are much higher than the standard double layer capacitance values. Higher values of C_{DL} observed in the present study are due to high electrochemical active surface.[28] Correlation of the values of EIM parameters such as R_{CT}, C_{DL}, etc. with the corrosion protection effect and with already reported results is a difficult task as results vary widely and are strongly influenced by the composition of the steel, corrosion environment, nature of coating (ES or EB) and top coat (if present).[4 6 27 29]

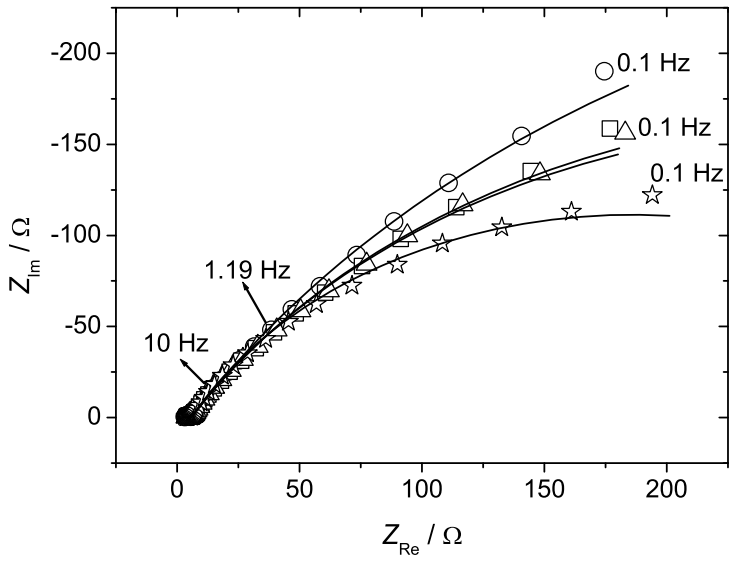

Figure 8. Nyquist diagrams of TIP-6 coated C45 steel electrodes recorded in 3.5 % NaCl at OCP (○), 24 h (□), 48 h (Δ) and 72 h (☆) of immersion time. Solid lines indicate the curve fitting.

Figure 8 shows Nyquist diagrams of TIP 6 coated C45 steel in 3.5 % NaCl recorded after different time intervals. The shape of the Nyquist diagrams is not much affected up to 72 hours. The R_{CT} values decrease with time but are still higher than with the uncoated electrodes. Bereket and coworkers[29] have also observed such a decrease in R_{CT} values for PANI coated 304-stainless steel electrodes. PANI film was generated by electropolymerization of aniline in acetonitrile containing tetrabutylammonium perchlorate and perchloric acid. We believe that soluble PANI DBSA protects C45 steel against corrosion through the formation of a passive layer which could be easily visualized as a gray oxide film underneath the PANI coating.[5]

Anodic Polarization Studies.—The corrosion potentials (E_{CORR}) and the corrosion currents (I_{CORR}) were determined from the Tafel slopes (β_a) of potentiodynamic measurements. The corrosion rate (C_R, in milliinches per year, MPY) was calculated from the following equation:

$$C_R = \frac{0.129 \cdot I_{CORR} \cdot (EW)}{A \cdot d}$$

where EW is the equivalent weight (g/equiv), A is the area (cm^2) and d is the density (g/mL). The E_{CORR} I_{CORR} β_a, R_P and C_R values for uncoated and PANI-coated C45 steel electrodes are summarized in **Table 2**.

Table 2. E_{CORR}, β_a, I_{CORR}, R_P and C_R values calculated from Tafel plots for bare and PANI-DBSA coated C45 steel electrode in 3.5 % NaCl.

Coating	[DBSA]/ [aniline]	$E_{CORR, SCE}$ (mV)	β_a (mV dec^{-1})	I_{CORR} (μA cm^{-2})	R_P (Ω)	C_R (MPY)
Uncoated	–	–571	40.0	98.80	92	40.12
TIP-5	5	–506	52.5	15.30	718	6.21
TIP-6	7	–499	47.4	13.79	805	5.60
TIP-7	10	–515	49.5	19.04	505	7.74

The corresponding Tafel plots for bare C45 steel and PANI-DBSA (different feed ratios of DBSA to aniline) coated electrodes are shown in **Figure 9**.

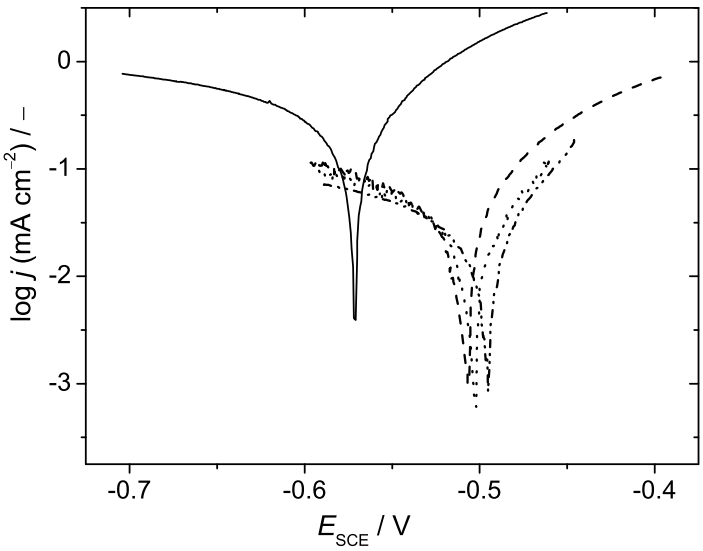

Figure 9. Tafel plots for bare (——), TIP-5 (•••••), TIP-6 (— •• — ••) and TIP-7 (— —) coated C45 steel electrodes recorded in 3.5 % NaCl at a scan rate of 5 mV/s.

The corrosion potential of the PANI coated electrode was anodically shifted by 66-72 mV compared to the bare electrode whereas the corrosion current and the corresponding corrosion rate are drastically reduced (Table 2). An anodic shift of 2 mV was reported for PANI-DBSA coated 08U-steel electrodes in 3.5 % NaCl by Pud and coworkers.[8] They cast emeraldine base form of PANI dissolved in NMP on the steel substrate and re-doped it with DBSA in xylene. However, they have found that PANI re-doped with CSA and DBSA increases the corrosion current in 3.5 % NaCl thereby showing an increase in corrosion rate. As mentioned in the preceding paragraph, corrosion protection mechanism is through formation of passive iron oxide layer which commences soon after the coating is applied. During this process, PANI-DBSA reduces from emeraldine-to-leucoemeraldine.[30] Reduced leucoemeraldine state of PANI easily undergoes air oxidation and transforms back to emeraldine state. Generally, at the operative potential of E_{SCE} = –0.3 to –0.7 V, PANI exists in leucoemeraldine state and therefore, any protection offered by PANI is due to the non-conducting leucoemeraldine state of PANI.

However, in situ UV-Vis spectroscopy exhibit band at 420 nm corresponding to radical cation at E_{SCE} = –0.2 V and cyclic voltammetry studies reveal that anion exchange between PANI-DBSA film and electrolyte solution is a slow process. Hence, we assume that at the operating potential (E_{SCE} = –0.3 to –0.7 V) and scan rate (5 mV s^{-1}) PANI-DBSA film is not completely reduced. The better corrosion protection performance of PANI-DBSA in our case can therefore be attributed to the stronger complexation of DBSA with the N-atoms of the polymer backbone. An increase in E_{CORR} up to 1650 mV was reported by several investigators.[5 31] The magnitude of potential shift and corrosion current strongly depends on the processing technology, composition of the steel and an insulating polymer top-coat.

The polarization resistances (R_P) calculated from Tafel plots (Table 2) are almost in agreement with the R_{CT} values calculated from impedance data (Table 1).* A significant increase in R_P after PANI coating confirms its protective nature against the corrosion of C45 steel. If the PANI-DBSA film is in completely reduced state then such an agreement between R_{CT} and R_P does not hold good. Hence, as mentioned earlier, corrosion protection is due to emeraldine PANI-DBSA salt and not due to leucoemeraldine. The E_{CORR} and I_{CORR} values are influenced by the ratio of DBSA to aniline in the feed. TIP-6 having a feed ratio of 10 shows better corrosion performance over the others which was also confirmed by EIM studies. As described under the sections of *in situ* UV-Vis spectroscopy and cyclic voltammetry, the hydrophobic nature of the long non-polar chain of DBSA and its strong complexation with PANI backbone hinders the rate of anion exchange which further reduces the ingress of hydrophilic (and pitting) Cl^- ions into the polymer film thereby enhancing the corrosion performance.

* The agreement between polarization resistance R_P (i.e. the slope of the current density vs. electrode potential curve) and the sum of all Ohmic components in the electrode impedance deduced from impedance measurements at the same electrode potential is expected, because at frequency zero the sum of all Ohmic components

Transmission Electron Microscopy (TEM).—**Figure 10** shows TEM images of PANI-DBSA at different feed ratios of DBSA to aniline.

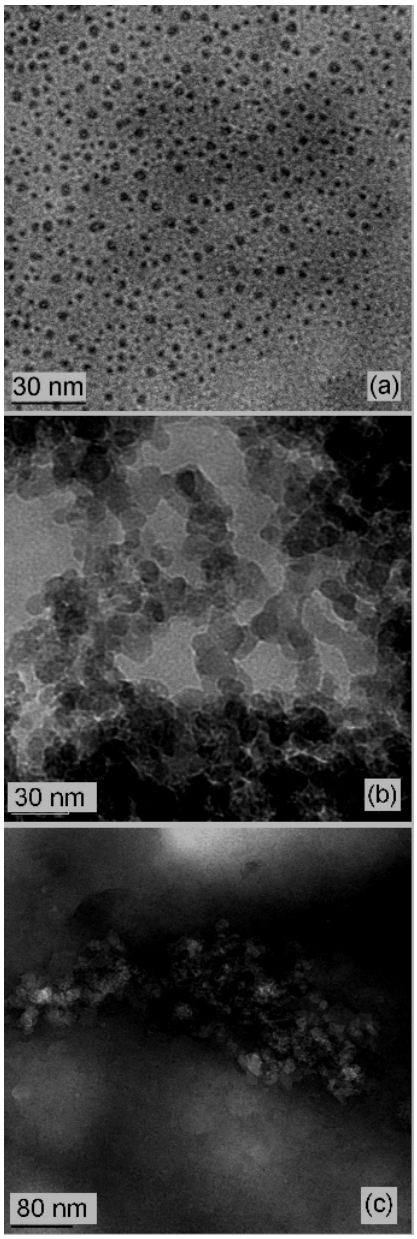

Figure 10. Transmission electron microscope images of TIP-5 (a), TIP-6 (b) and TIP-7 (c).

of the impedance is equal to said slope.[21] The relatively small contribution of the film resistance R_F and the solution resistance R_S results in the present case in the fairly good agreement between R_P and R_{CT}.

It is clear from the figures that the PANI particles are basically spherical in shape and their size is strongly influenced by the feed ratio of DBSA to aniline. When the ratio is 5, particles are organized in such a way which is normally exhibited by monolayers and the average particle size lies in the range of 1-7 nm. Increasing the feed ratio to 7 and then to 10 increases the average particle size to 8.5-15 nm and then to 20-30 nm respectively. The feed ratio of DBSA to aniline also influences the aggregation tendency of the PANI particles. In the case of TIP-6 and TIP-7 where the feed ratio is 7 and 10 respectively, the agglomeration tendency is higher leading to the formation group of spherical particles overlapping with each other. Yang and coworkers[32] have reported that TEM images of PANI-DBSA directly cast from the emulsion show entangled fibers of 1 μm width and a length of 1 mm. Nanocomposites of PANI-CSA and acrylic acid show rice grain shaped particles with 70 nm width and 120 nm length whereas electrochemically synthesized PANI-CSA exhibits agglomerated irregular shaped particles.[33] [34] The tendency of aggregation monitored in TEM images could be correlated to the bulk morphology (SEM) of the polymers. The well organized particles observed in the Figure 10a for TIP-5 leads to more ordered fibrillar morphology. Increasing tendency of aggregation as reflected from the TEM images for TIP-6 and TIP-7 (Figure 10b and 10c) leads to the formation of porous and compact polymer flakes, respectively.[14]

Electron diffraction (ED) patterns were recorded for several agglomerated areas observed in TEM images. At DBSA to aniline feed ratio of 5, ill defined ED patterns were observed indicating the presence of both crystalline (not shown in the figure) and amorphous (**Figure 11a**) regimes in the polymer. Well defined ED patterns having bright arcs of different lengths could be seen at DBSA to aniline feed ratio of 10 (**Figure 11b**).

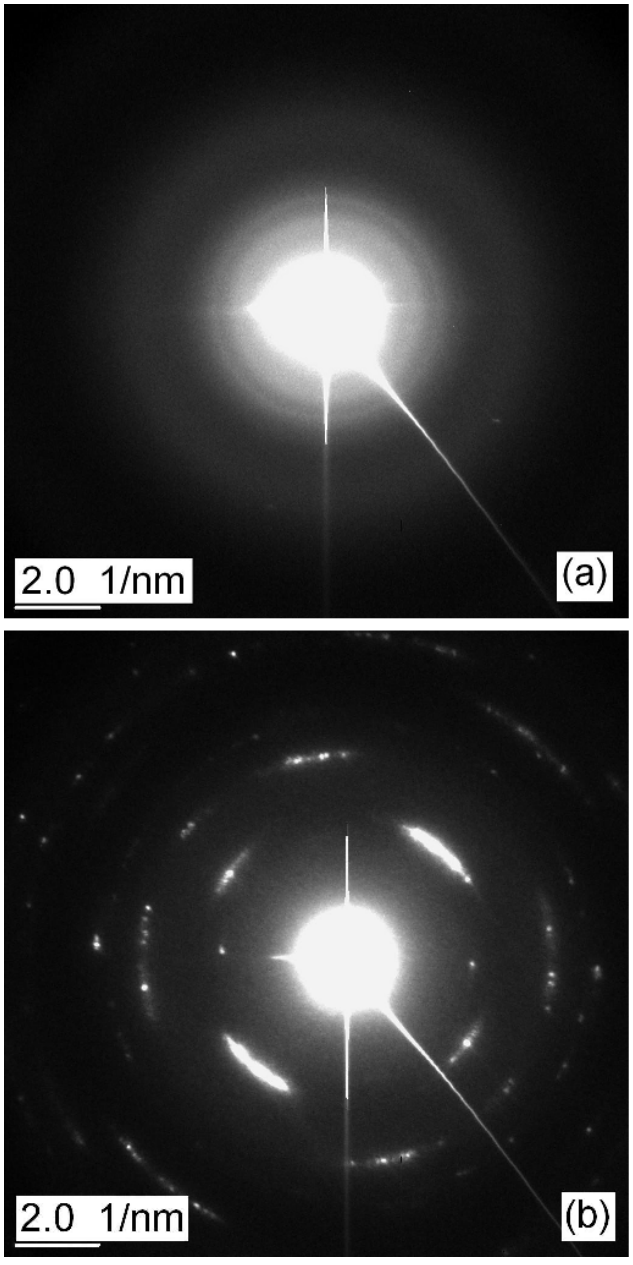

Figure 11. Electron diffraction patterns for selected agglomerated particles of TIP-5 (a) and TIP-7 (b).

Similar ED patterns were also observed for PANI-DBSA synthesized via an emulsion pathway and for an electrochemically synthesized PANI-CSA.[32 33] Such a pattern is attributed to an orthorhombic crystal structure. Further investigations to analyze the crystal structure of PANI-DBSA using ED patterns are underway.

Conclusions

PANI-DBSA synthesized by an inverse emulsion polymerization is completely soluble in chloroform in its pristine state and can be easily processed onto various metal substrates by simple drop, spin or spray coating technique. Solution state electronic absorption spectroscopy confirms the absence of interaction of chloroform with PANI backbone whereas 2:1 mixture of toluene+2-propanol forms hydrogen bonding with N atoms of PANI. PANI-DBSA in its emeraldine salt form offers better protection against corrosion of C45 steel which was confirmed by EIM where the charge transfer resistance for PANI coated electrode shows significant increase compared to the uncoated one. The anodic shift in the corrosion potential and lowering of the corrosion current for PANI-coated C45 steel electrode supports the improved anti-corrosion performance of this new soluble PANI. The improved corrosion protection of our samples is due to the hydrophobic nature of the non-polar chain of DBSA which hinders the permeability of aqueous anions into the polymer film. *In situ* UV-Vis spectroscopy and cyclic voltammetry of PANI-DBSA in neutral electrolytes confirms the slow rate of anion exchange. TEM images reveal that morphology of PANI at molecular level is different than that of the bulk morphology. However, the bulk morphology (SEM) could be correlated to the TEM images.

Acknowledgements

Financial support by the Deutsche Forschungsgemeinschaft (GRK 829/1) is gratefully acknowledged. We thank Dr. S. Schulze, Institute of Physics, TU Chemnitz for help in recording TEM images and ED patterns.

References

[1] P. Chandrashekhar, *Conducting Polymers, Fundamentals and Applications: A Practical Approach*, Kulwer Academic Publishers, Boston (1999).

[2] T. J. Skotheim, R. L. Elsenbaumer and J. R. Reynolds, *Handbook of Conducting Polymers*, Marcel Dekker, New York (1998**)**.

[3] P. S. Rao, D. N Sathyanarayana and T. Jeevananda, *Advanced Functional Molecules and Polymers*, ed. Nalwa., H.S.Vol.3, p. 79, Gordon and Breach Science (2001**)**.

[4] A. Cook, A. Gabriel and N. Laycock, *J. Electrochem. Soc*., **151**, B529 (2004).

[5] G. M. Spinks, A. J. Dominis, G. G. Wallace and D. E. Tallman, *J. Solid State Electrochem*., **6**, 85 (2002).

[6] A. T Ozyilmaz, M. Erbil and B. Yazici, *Curr. Appl. Phys*., **6**, 1 (2006).

[7] B. J. Wessling, *J. Corr. Sci. Eng.,* **1**, paper 15 (1999).

[8] A. A. Pud, G. S. Shapoval, P. Kamarchik, N. A. Ogurtsov, V. F. Gromovaya, I. E. Myronyuk and Yu. V. Kontsur, *Synth. Met*., **107**, 111 (1999).

[9] Y. Cao, P. Smith and A. J. Heeger, *Synth. Met.,* **48**, 91 (1992).

[10] Y. Haba, E. Segal, M. Narkis, G. I. Titelman and A. Siegmann, *Synth. Met*., **106**, 59 (1999).

[11] P. S. Rao, S. Subrahmanya and D. N. Sathyanarayana, *Synth. Met*., **128**, 311 (2002).

[12] P. S. Rao, S. Palaniappan and D. N. Sathyanarayana, *Macromolecules,* **35**, 4988 (2002).

[13] M. Sai Ram and S. J. Palaniappan, *J. Mater. Sci.,* **39**, 3069 (2004).

[14] S. Shreepathi and R. Holze, *Chem. Mater.,* **17**, 4078 (2005).

[15] A. A. Athawale, M. V. Kulkarni and V. V Chabukswar, *Mater. Chem. Phys*., **73**, 106 (2002).

[16] J. Stejskal, and I. Sapurina, *Pure Appl. Chem.,* **77**, 815 (2005).

[17] R. Mazeikiene, G. Niaura and A. Malinauskas, *Synth. Met.,* **139**, 89 (2003).

[18] M. C. Bernard, S. Joiret, A. H-L. Goff and P. D. Long, *J. Electrochem. Soc.,* **148**, B299 (2001).

[19] D. A. Buttry and M. D. Ward, *Chem. Rev.*, **92**, 1355 (1992).

[20] S. Mu, *Synth. Met.*, **143**, 259 (2004).

[21] R. Holze, *Bull. Electrochem.*, **10**, 56 (1994).

[22] N. Perez, *Electrochemistry and Corrosion Science,* p. 97, Kluwer Academic Publishers, Boston (2004).

[23] A. J. Bard and L. R. Fraulkner, *Electrochemical methods: Fundamentals and Applications,* p. 388, John Wiley & Sons, Inc. New York, (2001**)**.

[24] K. Belmokre, N. Azzouz, F. Kermiche, M. Wery and J. Pagetti, *Mater. Corr*., **49**, 108 (1998).

[25] T. Tuken, A. T. Ozyilmaz, B. Yazici, G. Kardas and M. Erbil, *Progress Org. Coatings,* **51**, 27 (2004).

[26] S. Sathiyanarayanan, S. Muthukrishnan, G. Venkatachari and D. C. Trivedi, *Progress Org. Coatings*, **53**, 297 (2005).

[27] J. Posdorfer and B. Wessling, *Fresenius J. Anal. Chem*., **367**, 343 (2000).

[28] E. Barsonkov, J. R. Macdonald, *Impedance Spectroscopy: Theory, Experiment and Applications*, 2nd Ed., Wiley-Interscience (2005).

[29] G. Bereket, E. Hür and Y. Sahin, *Appl. Surf. Sci.*, **252**, 1233 (2005).

[30] R. J. Holness, G. Williams, D. A. Worsley and H. N. McMurray, *J. Electrochem. Soc.*, **152**, B73 (2005).

[31] A. Mirmohseni and A. Oladegaragoze, *Synth. Met.*, **114**, 105 (2000).

[32] C. Y. Yang, P. Smith, A. J. Heeger, Y. Cao and J. E. Osterholm, *Polymer*, **35**, 1142 (1994).

[33] P. C. Innis, I. D. Norris, L. A. P. Kane-Maguire and G. G. Wallace, *Macromolecules*, **31**, 6521 (1998).

[34] P. A. McCarthy, J. Huang, S. C. Yang and H. L. Wang, *Langmuir,* **18**, 259 (2002).

.